Table IV. Intramolecular Bond Angles for **2**[a]

P(1)–Co–P(2)	99.36 (3)	C(2)–C(1)–P(1)	115.3 (2)
P(1)–Co–Co*	128.92 (3)	C(1)–C(2)–C(3)	113.5 (2)
P(2)–Co–Co*	131.55 (3)	C(2)–C(3)–P(2)	115.5 (2)
C(1)–P(1)–C(4)	100.8 (1)	C(8)–C(4)–C(9)	110.3 (3)
C(1)–P(1)–C(5)	100.7 (1)	C(8)–C(4)–P(1)	110.8 (2)
C(1)–P(1)–Co	119.0 (1)	C(9)–C(4)–P(1)	112.0 (2)
C(4)–P(1)–C(5)	101.8 (1)	C(10)–C(5)–C(11)	111.0 (3)
C(4)–P(1)–Co	115.7 (1)	C(10)–C(5)–P(1)	110.3 (2)
C(5)–P(1)–Co	116.1 (1)	C(11)–C(5)–P(1)	115.0 (2)
C(3)–P(2)–C(6)	100.6 (1)	C(13)–C(6)–C(12)	111.1 (3)
C(3)–P(2)–C(7)	100.9 (1)	C(13)–C(6)–P(2)	112.4 (2)
C(3)–P(2)–Co	119.30 (9)	C(12)–C(6)–P(2)	110.4 (2)
C(6)–P(2)–C(7)	102.0 (1)	C(14)–C(7)–C(15)	110.8 (3)
C(6)–P(2)–Co	116.6 (1)	C(14)–C(7)–P(2)	110.7 (2)
C(7)–P(2)–Co	114.7 (1)	C(15)–C(7)–P(2)	115.1 (2)
H(36)*–Co–H(36)	72 (3)	H(15)–C(9)–H(16)	109.49
H(36)*–Co–H(35)	72 (2)	H(15)–C(9)–H(14)	109.43
H(36)*–Co–P(1)	170 (2)	H(15)–C(9)–C(4)	109.51
H(36)*–Co–P(2)	89 (2)	H(16)–C(9)–H(14)	109.43
H(36)*–Co–Co*	43 (2)	H(16)–C(9)–C(4)	109.51
H(36)–Co–H(35)	71 (2)	H(14)–C(9)–C(4)	109.46
H(36)–Co–P(1)	104 (2)	H(17)–C(10)–H(18)	109.47
H(36)–Co–P(2)	132 (2)	H(17)–C(10)–H(19)	109.48
H(36)–Co–Co*	42 (2)	H(17)–C(10)–C(5)	109.49
H(35)–Co–P(1)	98 (1)	H(18)–C(10)–H(19)	109.46
H(35)–Co–P(2)	145.2 (2)	H(18)–C(10)–C(5)	109.46
H(35)–Co–Co*	43 (1)	H(19)–C(10)–C(5)	109.48
H(2)–C(1)–H(1)	109.47	H(20)–C(11)–H(21)	109.49
H(2)–C(1)–C(2)	107.98	H(20)–C(11)–H(22)	109.47
H(2)–C(1)–P(1)	108.00	H(20)–C(11)–C(5)	109.47
H(1)–C(1)–C(2)	107.98	H(21)–C(11)–H(22)	109.47
H(1)–C(1)–P(1)	107.99	H(21)–C(11)–C(5)	109.46
H(4)–C(2)–H(3)	109.47	H(22)–C(11)–C(5)	109.46
H(4)–C(2)–C(1)	108.46	H(23)–C(12)–H(24)	109.48
H(4)–C(2)–C(3)	108.46	H(23)–C(12)–H(25)	109.45
H(3)–C(2)–C(1)	108.44	H(23)–C(12)–C(6)	109.50
H(3)–C(2)–C(3)	108.45	H(24)–C(12)–H(25)	109.44
H(5)–C(3)–H(6)	109.46	H(24)–C(12)–C(6)	109.48
H(5)–C(3)–C(2)	107.95	H(25)–C(12)–C(6)	109.47
H(5)–C(3)–P(2)	107.97	H(27)–C(13)–H(26)	109.47
H(6)–C(3)–C(2)	107.95	H(27)–C(13)–H(28)	109.47
H(6)–C(3)–P(2)	107.97	H(27)–C(13)–C(6)	109.49
H(7)–C(4)–C(8)	107.86	H(26)–C(13)–H(28)	109.46
H(7)–C(4)–C(9)	107.84	H(26)–C(13)–C(6)	109.47
H(7)–C(4)–P(1)	107.84	H(28)–C(13)–C(6)	109.48
H(8)–C(5)–C(10)	106.65	H(29)–C(14)–H(31)	109.49
H(8)–C(5)–C(11)	106.66	H(29)–C(14)–H(30)	109.46
H(8)–C(5)–P(1)	106.66	H(29)–C(14)–C(7)	109.48
H(9)–C(6)–C(13)	107.60	H(31)–C(14)–H(30)	109.46
H(9)–C(6)–C(12)	107.59	H(31)–C(14)–C(7)	109.48
H(9)–C(6)–P(2)	107.61	H(30)–C(14)–C(7)	109.46
H(10)–C(7)–C(14)	106.54	H(34)–C(15)–H(32)	109.49
H(10)–C(7)–C(15)	106.54	H(34)–C(15)–H(33)	109.48
H(10)–C(7)–P(2)	106.54	H(34)–C(15)–C(7)	109.49
H(12)–C(8)–H(11)	109.49	H(32)–C(15)–H(33)	109.45
H(12)–C(8)–H(13)	109.47	H(32)–C(15)–C(7)	109.46
H(12)–C(8)–C(4)	109.49	H(33)–C(15)–C(7)	109.45
H(11)–C(8)–H(13)	109.46	Co–H(35)–Co*	93 (3)
H(11)–C(8)–C(4)	109.47	Co–H(36)–Co*	96 (3)
H(13)–C(8)–C(4)	109.46		

[a] Angles are in degrees. Estimated standard deviations in the least significant figure are given in parentheses.

in the usual manner using a continuous θ–2θ scan with fixed backgrounds. Data were reduced to a unique set of intensities and associated σ's in the usual manner. An absorption correction was made, with maximum and minimum values of 0.925 and 0.876, respectively.

Full-matrix refinement of the non-hydrogen atoms followed by a difference Fourier map located some of the hydrogen atoms. Although the bridging hydride was present in this map, it was left out of the initial refinement. After several cycles, all hydrogen atoms "behaved" normally and a difference Fourier map was generated. In it there was one large peak (0.5 e/Å^3) in a proper position to bridge the two Co atoms. All other peaks within bonding distance of the Co atoms were less than 0.25 e/Å^3 in intensity. Although there was a peak on the 2-fold axis, it was 14th on the list, with an intensity of 0.21 e/Å^3, and was apparently too close to the center of the Co–Co bond to be a hydride. When the hydride was introduced at the 2-fold site and refinement concluded, it behaved properly although the thermal parameter is considerably higher than those of any of the remaining hydrogen atoms.

Acknowledgment. Financial support from the NATO International Collaborative Grants Program and the Natural Sciences and Engineering Research Council of Canada (NSERC) is gratefully acknowledged. We thank Phil Matsunaga (Berkeley) and Dr. Warren Piers (Caltech) for experimental assistance.

Supplementary Material Available: (a) For the data set at 21 °C, tables of crystal and diffractometer data, U values, torsion or conformational angles, and least-squares planes for **2**, (b) for the data set at −155 °C, a full report on **2** of all details concerning crystal and diffractometer data and tables of fractional coordinates, anisotropic thermal parameters, and bonded distances and angles for **2**, and (c) VERSORT, ORTEP, and space filling model drawings for **2** (42 pages); listings of observed and calculated structure factor amplitudes for **2** at 21 and −155 °C (38 pages). Ordering information is given on any current masthead page.

Contribution from the Department of Chemistry,
University of Alabama at Birmingham,
Birmingham, Alabama 35294

Reactivity of μ-$Me_2NB_2H_5$ toward the As–N Bond

D. K. Srivastava, L. K. Krannich,* and C. L. Watkins

Received November 12, 1990

During our studies on the reactivity of $BH_3\cdot THF$ with mono-, bis-, and tris(dimethylamino) methyl-substituted arsines,[1-3] we observed that μ-$Me_2NB_2H_5$ formed whenever the $BH_3\cdot THF$ was in excess relative to the number of available nitrogen base sites. Decomposition of the N–B-bonded adducts of the aminoarsines gives Me_2NBH_2, which reacts with the excess $BH_3\cdot THF$ to yield μ-$Me_2NB_2H_5$.

This route to the μ-$Me_2NB_2H_5$ is analogous to the nearly quantitative synthesis of Burg and Randolph,[4] wherein the Me_2NBH_2 that is formed from the reaction of Me_2NH with B_2H_6 is reacted with additional B_2H_6. A variation on this reaction was also reported by Spielman and was used by us in our synthesis of μ-$Me_2NB_2H_5$.[5,6] Several other synthetic routes to μ-$Me_2NB_2H_5$ have been reported.[7-9]

There is a somewhat limited literature on the reactivity of μ-$Me_2NB_2H_5$ with group 15 bases.[4,10-15] In almost all cases, the products are simple 1:1 adducts. The work of Hahn and Schaeffer established that the products from the reactions with NH_3, $MeNH_2$, Me_2NH, and Me_3N are substituted diborazanes.[10] The adducts formed with Me_3N, pyridine, Me_3P, Me_2PH, and $MePH_2$ were shown by Burg and Sandhu to exist with reversible disso-

---

(1) Kanjolia, R. K.; Krannich, L. K.; Watkins, C. L. *Inorg. Chem.* **1985**, *24*, 445.
(2) Kanjolia, R. K.; Krannich, L. K.; Watkins, C. L. *J. Chem. Soc., Dalton Trans.* **1986**, 2345.
(3) Watkins, C. L.; Krannich, L. K.; Srivastava, D. K.; Kanjolia, R. K. *Coord. Chem. Rev.*, invited paper, main group coordination chemistry issue, in press.
(4) Burg, A. B.; Randolph, C. L. *J. Am. Chem. Soc.* **1949**, *71*, 3451.
(5) Spielman, J. R. *J. Chem. Educ.* **1970**, *47*, 225.
(6) Burg, A. B. *J. Am. Chem. Soc.* **1952**, *74*, 1340.
(7) Keller, P. C. *J. Am. Chem. Soc.* **1969**, *91*, 1231.
(8) Schwartz, L. D.; Keller, P. C. *J. Am. Chem. Soc.* **1972**, *94*, 3015.
(9) Keller, P. C. *Synth. Inorg. Met.-Org. Chem.* **1973**, *3*, 307.
(10) Hahn, G. A.; Schaeffer, R. S. *J. Am. Chem. Soc.* **1964**, *86*, 1503.
(11) Burg, A. B.; Sandhu, J. S. *Inorg. Chem.* **1965**, *4*, 1467.
(12) Zhigach, A. F.; Svitsyn, R. A.; Sobolev, E. S. *J. Gen. Chem. USSR (Engl. Transl.)* **1973**, *43*, 1541.
(13) Keller, P. C. *Inorg. Chem.* **1982**, *21*, 444.
(14) Molinelli, R.; Smith, S. R.; Tanaka, J. *J. Chem. Soc., Dalton Trans.* **1972**, 1363.
(15) Schlesinger, H. I.; Ritter, D. M.; Burg, A. B. *J. Am. Chem. Soc.* **1938**, *60*, 2297.

Table I. NMR Spectral Data

compd	*T*, °C	^{11}B NMR, ppm	^{13}C NMR, ppm	^{1}H NMR, ppm
I	-60	-1.4 (BH_2) -10.5 (BH_3)	53.89 (-NMe_2BH_3) 43.55 (>$AsNMe_2$) 11.75 (Me_2As-)	2.48 (>$AsNMe_2$) 2.33 (-NMe_2BH_3) 0.36 (Me_2As-)
II, III[a]	-80	-9.3 (BH_3) 0.0 (BH_2)	54.30, 53.32, 45.89, 44.14 38.76 13.63, 13.58 (MeAs<)	2.52, 2,47 2.45, 2.19 0.85 (MeAs<)
IV	-70	0.9 (BH_2) -10.2 (BH_3)	54.09 (-NMe_2BH_3) 43.51, 41.23	2.55 (-NMe_2BH_3) 2.49, 2.27
$Me_2AsAsMe_2$	room temp		5.94	0.96
Me_2AsNMe_2	room temp		41.92 (Me_2N), 9.70 (Me_2As)	2.42 (Me_2N), 0.79 (Me_2As)
Me_2AsH	room temp		1.43	2.39 (AsH), 0.77 (Me_2As)
$(MeAs)_5$	room temp		6.81, 5.23, 3.78	1.54, 1.50, 1.48
$MeAs(NMe_2)_2$	room temp		42.76 (Me_2N), 12.39 (MeAs)	2.64 (Me_2N), 0.96 (MeAs)
$As(NMe_2)_3$	room temp		39.72	2.59
$[Me_2NBH_2]_2$	room temp	5.2	51.68	2.24
$(Me_2N)_2BH$	room temp	27.3[b]	40.95	2.62
μ-$Me_2NB_2H_5$	room temp	-17.5[c]	50.91	2.08 (Me_2N), 1.64 (BH_2), 0.6 (BH)
$Me_2NHBH_2NMe_2BH_3$	room temp	-13.0 (BH_3),[d] 2.0 (BH_2)[e]	52.43 (Me_2N<), 42.58 (Me_2NH)	4.95 (>NH), 2.28 (Me_2N<), 2.01 (BH_2) 1.97 (BH_3), 1.81 (Me_2NH)
Me_2NBH_2	-70	37.9	42.39	
$Me_2NBH_2{\cdot}HNMe_2$	-70	3.2	52.8 (Me_2N) 43.8 (Me_2NH)	

[a] Individual resonance assignments for II and III could not be made. [b] Doublet, $^{1}J(BH) = 130$ Hz. [c] Terminal, $^{1}J(BH) = 130$ Hz; bridging, $^{1}J(BH) = 31.7$ Hz. [d] $^{1}J(BH) = 108$ Hz. [e] $^{1}J(BH) = 94$ Hz.

ciation.[11] On standing or at elevated temperatures, an irreversible decomposition reaction occurs to yield $[Me_2NBH_2]_2$ and the BH_3 adduct of the base. With the weak base $MePH_2$, data do not establish whether an adduct is formed at low temperature or the solid solution is made up of equilibrium amounts of the components.[11] At elevated temperatures, some decomposition occurs.

There have been very few reported reactions of μ-$Me_2NB_2H_5$ with multiple Lewis base site containing molecules. With the 1,1- and 1,2-dimethylhydrazines, μ-$Me_2NB_2H_5$ readily reacts with evolution of hydrogen and formation of $[Me_2NBH_2]_2$ and supposedly the respective hydrazinoboranes.[12] Evidence for the hydrazinoboranes is quite limited. With methyl isocyanate the reaction is viewed as giving an initial N-B-bonded 1:1 adduct with a subsequent hydroboration reaction leading to the final product.[14] A unique asymmetric cleavage reaction occurs with tetramethyl-*o*-phenylenediamine to give an ionic product.[13]

This paper describes the mode of reactivity of μ-$Me_2NB_2H_5$ with the multiple Lewis base site compounds Me_2AsNMe_2, $MeAs(NMe_2)_2$, and $As(NMe_2)_3$. The reactions were followed by temperature-dependent ^{1}H, ^{11}B, and ^{13}C NMR spectroscopy. This study indicates that reaction occurs at very low temperature to give a 1:1 adduct in each case. The decomposition pathways of these adducts have been elucidated.

Results and Discussion

Reaction of μ-$Me_2NB_2H_5$ with Me_2AsNMe_2. The reaction of μ-$Me_2NB_2H_5$ with Me_2AsNMe_2 in a 1:1 mole ratio occurs to give a 1:1 N-B-bonded adduct, $Me_2AsNMe_2{\cdot}BH_2NMe_2BH_3$ (I), which is in equilibrium with a mixture of unreacted μ-$Me_2NB_2H_5$ and Me_2AsNMe_2 (eq 1). See Table I for NMR spectral data. This results in spectral line width broadening in the ^{11}B NMR spectrum (Figure 1, -90 °C spectrum). At -80 °C adduct decomposition begins with the appearance of peaks in the NMR spectrum assignable to $Me_2NHBH_2NMe_2BH_3$,[10] $(Me_2NBH_2)_2$,[2] and $Me_2AsAsMe_2$[2,16] (eqs 2-4). By analogy to the $BH_3{\cdot}THF$ reactions with Me_2AsNMe_2,[1-3] we postulate that I decomposes to $Me_2NBH_2NMe_2BH_2$ and Me_2AsH (eq 2). The former dimerizes to $[Me_2NBH_2]_2$ (eq 4), and Me_2AsH reacts with I to give $Me_2AsAsMe_2$ and the diborazane $Me_2NHBH_2NMe_2BH_3$ (eq 3). This is analogous to the reaction of Me_2AsH with $Me_2AsNMe_2{\cdot}BH_3$, which yields $Me_2AsAsMe_2$ and $Me_2NH{\cdot}BH_3$.[2,16] Me_2AsH can also react with available Me_2AsNMe_2 to give $Me_2AsAsMe_2$ (eq 5) and Me_2NH,[16] with would react with μ-$Me_2NB_2H_5$ to give the diborazane (eq 6).[10]

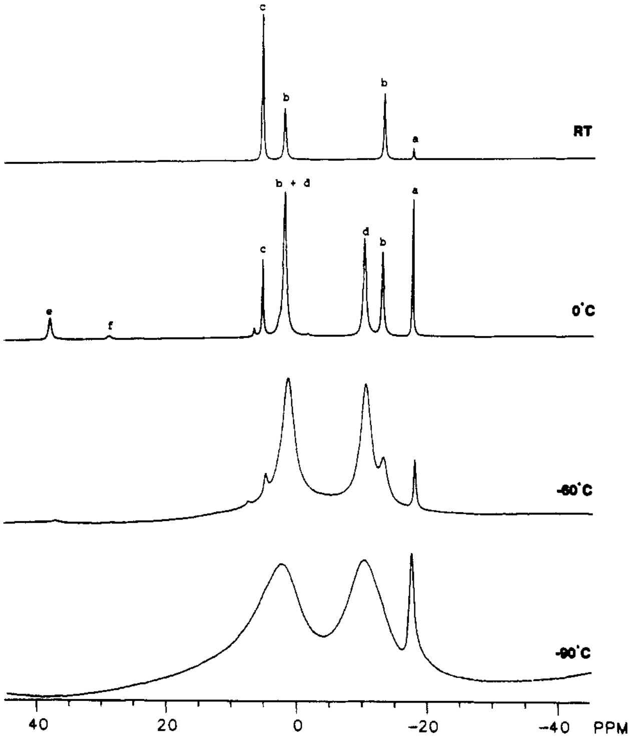

Figure 1. Selected temperature-dependent ^{11}B NMR spectra of the 1:1 μ-$Me_2NB_2H_5$/Me_2AsNMe_2 reaction system (RT = room temperature): (a) μ-$Me_2NB_2H_5$; (b) $Me_2NH{\cdot}BH_2NMe_2BH_3$; (c) $[Me_2NBH_2]_2$; (d) I; (e) Me_2NBH_2; (f) $(Me_2N)_2BH$.

$$Me_2AsNMe_2 + \mu\text{-}Me_2NB_2H_5 \leftrightarrow Me_2AsNMe_2{\cdot}BH_2NMe_2BH_3 \quad (1)$$

$$Me_2AsNMe_2{\cdot}BH_2NMe_2BH_3 \rightarrow Me_2AsH + Me_2NBH_2NMe_2BH_2 \quad (2)$$

$$Me_2AsH + Me_2AsNMe_2{\cdot}BH_2NMe_2BH_3 \rightarrow Me_2AsAsMe_2 + Me_2NHBH_2NMe_2BH_3 \quad (3)$$

$$Me_2NBH_2NMe_2BH_2 \rightarrow [Me_2NBH_2]_2 \quad (4)$$

$$Me_2AsH + Me_2AsNMe_2 \rightarrow Me_2AsAsMe_2 + Me_2NH \quad (5)$$

$$Me_2NH + \mu\text{-}Me_2NB_2H_5 \rightarrow Me_2NHBH_2NMe_2BH_3 \quad (6)$$

---

(16) Gupta, V. K.; Krannich, L. K.; Watkins, C. L. *Inorg. Chem.* **1986**, *25*, 2553.

By −60 °C, peaks assignable to I, μ-$Me_2NB_2H_5$, $Me_2NHBH_2NMe_2BH_3$, $[Me_2BH_2]_2$, $Me_2AsAsMe_2$, Me_2AsH, and a trace of Me_2NBH_2 are observed in the spectra. See Figure 1, −60 °C spectrum, for the ^{11}B spectrum. As the temperature is increased (−40 to 0 °C), the appearance of peaks associated with $(Me_2N)_2BH$[3] (trace) and an increase in those assigned to Me_2NBH_2[2] suggest that there is a second decomposition route for I (Figure 1, 0 °C). This route is analogous to the decomposition pathway of the 1:1 amine/μ-$Me_2NB_2H_5$ adducts[4,10,11] and produces Me_2NBH_2 and $Me_2AsNMe_2{\cdot}BH_3$, which decomposes to Me_2AsH and Me_2NBH_2 (eqs 7 and 8).[2,3] Me_2AsH reacts are previously described (eqs 3 and 5), and Me_2NBH_2 can either dimerize to $[Me_2NBH_2]_2$ (eq 9) or react with available Me_2AsNMe_2 to give more Me_2AsH and $(Me_2N)_2BH$ (eq 10).[3]

$$Me_2AsNMe_2{\cdot}BH_2NMe_2BH_3 \rightarrow Me_2AsNMe_2{\cdot}BH_3 + Me_2NBH_2 \quad (7)$$

$$Me_2AsNMe_2{\cdot}BH_3 \rightarrow Me_2AsH + Me_2NBH_2 \quad (8)$$

$$2Me_2NBH_2 \rightarrow [Me_2NBH_2]_2 \quad (9)$$

$$Me_2NBH_2 + Me_2AsNMe_2 \rightarrow Me_2AsH + (Me_2N)_2BH \quad (10)$$

Additional support for these latter reactions is suggested by the fact that systems in which the μ-$Me_2NB_2H_5$:Me_2AsNMe_2 mole ratio is 1:>1 yield greater amounts of $(Me_2N)_2BH$. The final composition in the product mixture for the 1:1 mole ratio system is a 1:1:1 ratio of $Me_2AsAsMe_2$, $[Me_2NBH_2]_2$, and $Me_2NHBH_2NMe_2BH_3$ and a trace of μ-$Me_2NB_2H_5$ remaining (Figure 1, room temperature).

Reaction of μ-$Me_2NB_2H_5$ with $MeAs(NMe_2)_2$. The reaction of μ-$Me_2NB_2H_5$ with $MeAs(NMe_2)_2$ (1:1 mole ratio) at −90 °C gives spectral peaks assignable to an equilibrium mixture of starting materials: $MeAs(NMe_2)NMe_2{\cdot}BH_2NMe_2BH_3$ (II) and $MeAs(NMe_2{\cdot}BH_3)NMe_2{\cdot}BH_2NMe_2$ (III) (II:III mole ratio is 1:1). III probably arises via the dissociation of II to give a species with the BH_3 bound to the most basic Me_2N moiety. From −80 to −60 °C, these adducts decompose, as evidenced by the appearance of peaks assignable to $(Me_2N)_2BH$, $Me_2NHBH_2NMe_2BH_3$, $Me_2NBH_2{\cdot}HNMe_2$, and $(MeAs)_5$[17] and numerous peaks associated with uncharacterized As–As-bonded intermediates.[17] These intermediates can react with As–H- and As–N-bonded species in solution to lead to the formation of $(MeAs)_5$ and Me_2NH.[17]

Above −60 °C, line width broadening in the Me_2N region of the spectra suggests Me_2NH exchange between $Me_2NBH_2{\cdot}NHMe_2$, μ-$Me_2NB_2H_5$, and $Me_2NHBH_2NMe_2BH_3$. With increasing temperature, peaks assignable to $Me_2NBH_2{\cdot}HNMe_2$ and μ-$Me_2NB_2H_5$ decrease in intensity as those associated with $Me_2NHBH_2NMe_2BH_3$ and $[Me_2NBH_2]_2$ increase in intensity. These results suggest that μ-$Me_2NB_2H_5$ and Me_2NBH_2 compete for the bound Me_2NH. From 0 °C to room temperature, the peaks associated with $Me_2NHBH_2NMe_2BH_3$ and $MeAs(NMe_2)_2$ decrease in intensity as those assigned to $[Me_2NBH_2]_2$ and $(MeAs)_5$ increase in intensity. This implies that $Me_2NHBH_2NMe_2$ and $MeAs(NMe_2)_2$ compete for the bound BH_3. Decomposition of the BH_3 adduct of $MeAs(NMe_2)NMe_2$ provides an alternate route to $(MeAs)_5$.[3] The final product mixture is composed of $(MeAs)_5$ and a 0.3:1:1 mole ratio of $(Me_2N)_2BH$:$[Me_2NBH_2]_2$:$Me_2NHBH_2NMe_2BH_3$.

Reaction of μ-$Me_2NB_2H_5$ with $As(NMe_2)_3$. In the reaction of μ-$Me_2NB_2H_5$ with $As(NMe_2)_3$ (1:1 mole ratio), peaks assignable to $(Me_2N)_2As(NMe_2{\cdot}BH_2NMe_2BH_3)$ (IV) are observed at −80 °C, although there are considerable amounts of unreacted μ-$Me_2NB_2H_5$ and $As(NMe_2)_3$ in solution. By −70 °C, additional amounts of IV have formed and significant adduct decomposition has occurred, as evidenced by the observation of peaks assignable to $[Me_2NBH_2]_2$, Me_2NBH_2, $Me_2NHBH_2NMe_2BH_3$, Me_2NH, and $(Me_2N)_2BH$ in the NMR spectra. The decomposition process continues until −40 °C, when all the peaks associated with IV have disappeared. The nature of the decomposition products suggests that, by analogy to the $MeAs(NMe_2)_2$ results, the reaction mixture probably contains both IV and an uncharacterized adduct that contains two B–N bonds, $Me_2NAs(NMe_2{\cdot}BH_3)NMe_2{\cdot}BH_2NMe_2$. This adduct would arise from an intramolecular competition of the available nitrogen base sites for the BH_3 in IV, with the BH_3 in exchange between these nitrogen base sites. Decomposition of IV and its involvement in oligomerization reactions yield $[Me_2NBH_2]_2$ and $Me_2NHBH_2NMe_2BH_3$. Decomposition of the other adduct, $Me_2NAs(NMe_2{\cdot}BH_3)NMe_2{\cdot}BH_2NMe_2$, should yield $(Me_2N)_2BH$ and As–H-bonded intermediates. All these intermediates, which would be very reactive, should readily undergo condensation reactions with the adducts, the unreacted $As(NMe_2)_3$, and any other As–N-bonded intermediates.[3,17] Line width broadenings in the ^1H and ^{13}C NMR spectra suggest Me_2N moiety exchange involving the arsenic-containing intermediates, Me_2NH, $As(NMe_2)_3$, $Me_2NHBH_2NMe_2BH_3$, and $(Me_2N)_2BH$.

From −40 °C to room temperature, condensation, chaining, and cross-linking continue, with darkening of the solution followed by precipitation of elemental As and plating out of an arsenic mirror on the walls of the NMR tube. As this occurs, peaks assignable to $Me_2NHBH_2NMe_2BH_3$ and $As(NMe_2)_3$ decrease in intensity as those associated with $[Me_2NBH_2]_2$ and $(Me_2N)_2BH$ increase. These results suggest that $Me_2NHBH_2NMe_2BH_3$ acts as a source of available BH_3 for reaction with $As(NMe_2)_3$. On the basis of results from the reactions of BH_3 with $As(NMe_2)_3$,[3] there are an extensive series of reactions that can occur to lead to elemental arsenic, $(Me_2N)_2BH$, and $[Me_2NBH_2]_2$ from such an initial 1:1 BH_3 adduct formed with $As(NMe_2)_3$. The final product composition is made up of elemental As, Me_2NH, and a 0.1:1:1 mole ratio of $[Me_2NBH_2]_2$:$Me_2NHBH_2NMe_2BH_3$:$(Me_2N)_2BH$. $[Me_2NBH_2]_2$ is a minor component.

This study indicates that for 1:1 mole ratio reaction systems μ-$Me_2NB_2H_5$ readily reacts with aminoarsines to form exclusively 1:1 B–N-bonded adducts. This is consistent with the earlier reports on the reactivity of μ-$Me_2NB_2H_5$ toward amines and phosphines[4,10,11] and with our earlier competition studies;[18] i.e., the As–N base pair behaves as an amine nitrogen in reaction with $BH_3{\cdot}THF$. All the 1:1 B–N-bonded adducts are unstable and undergo decomposition to yield As–As-bonded products, $[Me_2NBH_2]_2$, $Me_2NHBH_2NMe_2BH_3$, and $(Me_2N)_2BH$. These decomposition results are in contrast to those previously reported for μ-$Me_2NB_2H_5$ adducts of amines and phosphines, which yield $[Me_2NBH_2]_2$ and a base/BH_3 adduct. Our results suggest that the aminoarsine/μ-$Me_2NB_2H_5$ adducts decompose at −80 °C to $[Me_2NBH_2]_2$ and highly reactive As–H-bonded species. The latter readily react with the original μ-$Me_2NB_2H_5$ adduct to product the diborazane $Me_2NHBH_2NMe_2BH_3$ and an As–As-bonded species. In the Me_2AsNMe system, this produces $Me_2AsAsMe_2$. In the $MeAs(NMe_2)_2$ and $As(NMe_2)_3$ systems, the As–H-bonded intermediates react at low temperature with any unreacted aminoarsine or the B–N-bonded aminoarsine adducts to give As–As-bonded oligomers, which ultimately lead to $(MeAs)_5$ and elemental arsenic in the respective systems. This is consistent with our results from the reactions of $BH_3{\cdot}THF$ with aminoarsines.[2,3] Only in the Me_2AsNMe_2 system are peaks associated with the initial As–H-bonded decomposition product, Me_2AsH, observed in the NMR spectrum.

The relative distribution of B–N-bonded products is dependent upon the mole ratio of μ-$Me_2NB_2H_5$ to available nitrogen base sites. With an increasing mole ratio of nitrogen base sites or aminoarsine in the system, there is increased formation of $(Me_2N)_2BH$. Spectral data suggest that the 1:1 adducts in the $MeAs(NMe_2)_2$ and $As(NMe_2)_3$ cases probably dissociate to species that have a BH_3 bonded to one nitrogen and a BH_2NMe_2 group bonded to the other nitrogen base site(s) of the aminoarsine. The decomposition of these BH_3/BH_2NMe_2-bonded adducts provides one pathway to $(Me_2N)_2BH$. Also, whenever there is an available unbound nitrogen base site in the presence of

---

(17) Gupta, V. K.; Krannich, L. K.; Watkins, C. L. *Inorg. Chim. Acta* **1987**, *126*, 173.

(18) Kanjolia, R. K.; Srivastava, D. K.; Watkins, C. L.; Krannich, L. K. *Inorg. Chem.* **1989**, *28*, 3341.

$Me_2NHBH_2NMe_2BH_3$, the nitrogen base site in the parent aminoarsine effectively competes for the BH_3 bound in the diborazane. This competition leads to dissociation of the diborazane and formation of a BH_3 adduct of the aminoarsine. $[Me_2NBH_2]_2$ forms and BH_3/aminoarsine adduct decomposition yields $(Me_2N)_2BH$ and an alternate route to the As–As-bonded products. These results are consistent with those obtained from our study of the analogous BH_3/aminoarsine systems with varying stoichiometry.[3]

Experimental Section

General Data. Due to the nature of the materials, standard high-vacuum-line techniques and a nitrogen-filled dri-lab (Vacuum Atmospheres Model HE-43 Dri-Lab equipped with a Model HE-493 Dri-Train) were used for the storage and manipulation of all compounds. Me_2AsNMe_2 (74 °C/108 mmHg), $MeAs(NMe_2)_2$ (63 °C/50 mmHg), and $As(NMe_2)_3$ (55–57 °C/10 mmHg) were synthesized by the reaction of Me_2AsCl, $MeAsCl_2$, and $AsCl_3$, respectively, with a stoichiometric excess of Me_2NH.[19] Me_2AsCl (106 °C)[20] and $MeAsCl_2$ (61–63 °C/50 mmHg)[21] were synthesized by previously reported methods. The aminoarsines were purified by distillation on a spinning-band column, and their purity was checked by ^1H and ^{13}C NMR spectroscopy. μ-$Me_2NB_2H_5$ was synthesized by the procedure described by Spielman.[5] Toluene-d_8 was purchased from Wilmad Glass Co. and stored over molecular sieves. ^1H, ^{11}B, and ^{13}C NMR spectra were recorded on a GE (Nicolet) 300-MHz multinuclear FT NMR spectrometer operating at 300.1, 96.3, and 75.4 MHz, respectively. ^1H and ^{13}C NMR chemical shifts were measured with respect to Me_4Si as an internal reference. The ^{11}B NMR chemical shifts were measured relative to the signal of $BF_3{\cdot}OEt_2$, high-field shifts being taken as negative. The ^{11}B and ^{13}C NMR spectra were obtained under broadband ^1H decoupling. Thus, all ^{11}B and ^{13}C NMR resonances were observed as singlets. Additionally, some ^{11}B NMR spectra were obtained under coupled conditions to determine the magnitude of $^1J(BH)$. NMR spectral data were independently determined in this laboratory in toluene-d_8 solution on prepurified or synthesized compounds identified in the reaction mixtures. The NMR data for all the adducts and prepurified or synthesized compounds are given in Table I.

General Reaction of μ-$Me_2NB_2H_5$ with Aminoarsines. J. Young VNMR tubes were charged with 1 mmol of the aminoarsine in 3.0 mL of toluene-d_8, attached to the vacuum line, cooled to −115 °C (liquid-nitrogen/ethanol slush), and degassed. The vapor of μ-$Me_2NB_2H_5$ were treated as an ideal gas, and the appropriately measured amount of μ-$Me_2NB_2H_5$ was condensed onto the toluene solution. The sealed NMR tube was gently agitated and inserted into the precooled (−95 °C) probe of the spectrometer. The reactions were followed at 10-deg temperature intervals (−95 to +25 °C) by ^1H, ^{11}B, and ^{13}C NMR spectroscopy.

---

(19) Modritzer, K. *Chem. Ber.* **1959**, *92*, 2637.
(20) Steinkopf, W.; Mieg, W. *Chem. Ber.* **1920**, *53*, 1013.
(21) Dehn, W. M.; Wilcox, B. B. *Am. Chem. J.* **1906**, *35*, 1.

Contribution from the Department of Chemistry,
University of Houston, Houston, Texas 77204-5641

Electrochemistry of (Octaethylporphinato)cobalt(II), (OEP)Co, under a Carbon Monoxide Atmosphere. Electrogeneration and Characterization of $[(OEP)Co^{III}(CO)]^+$

Y. Hu, B. C. Han, L. Y. Bao, X. H. Mu, and K. M. Kadish*

Received December 20, 1990

The first example for carbon monoxide binding to a singly oxidized cobalt porphyrin was recently reported.[1] The investigated complex was $[(TPP)Co(CO)]^+$ (where TPP = the dianion of tetraphenylporphyrin), which was electrogenerated from (TPP)Co by cyclic voltammetry in CH_2Cl_2 containing 0.1 M tetra-*n*-butylammonion perchlorate (TBAP) under a CO atmosphere and characterized by thin-layer spectroelectrochemistry. Under these solution conditions, the initial Co(II) derivative undergoes three oxidations, which are represented as shown in eqs 1–3.

$$(TPP)Co + CO \rightleftarrows [(TPP)Co(CO)]^+ + e^- \tag{1}$$

$$[(TPP)Co(CO)]^+ \rightleftarrows [(TPP)Co]^{2+} + e^- + CO \tag{2}$$

$$[(TPP)Co]^{2+} \rightleftarrows [(TPP)Co]^{3+} + e^- \tag{3}$$

The UV–visible spectrum of $[(TPP)Co(CO)]^+$ has bands at 431, 545, and 582 nm. An identical spectrum was obtained for electrogenerated $[(TPP)Co(CH_3CN)]^+$ in CH_3CN, and on the basis of this similarity, a Co(III) oxidation state was assigned for the carbon monoxide complex.[1] However, a CO vibration band of $[(TPP)Co(CO)]^+$ was not reported nor was a diagnostic π-cation-radical marker band of singly or doubly oxidized (TPP)Co under CO presented.

Infrared π-cation-radical bands have been reported at 1290 cm^{-1} for $(TPP)Co(SbCl_6)$[2] and at 1298 cm^{-1} for electrogenerated $[(TPP)Co]^{2+}$ in CH_2Cl_2, 0.1 M TBAP.[3] The $(TPP)Co(SbCl_6)$ sample[2] appears to be Co(II) π cation radical, but both electrochemically[3,4] and photochemically[5] generated $[(TPP)Co]^+$ seem to contain a Co(III) central metal ion in solutions of CH_2Cl_2, CH_2Br_2, or other chlorinated solvents. Under these solution conditions, a π-cation-radical band would thus be expected to appear upon oxidation of $[(TPP)Co(CO)]^+$ to $[(TPP)Co^{III}]^{2+}$ (eq 2). However, this band would be difficult to observe, since the second and third oxidations of (TPP)Co are virtually overlapped in potential under a CO atmosphere[1] and this results in a direct conversion of $[(TPP)Co(CO)]^+$ to $[(TPP)Co]^{3+}$, the latter of which is a Co(III) dication.

Octaethylporphyrin (OEP) π-cation-radical marker bands occur between 1540 and 1570 cm^{-1} in the infrared region[2,6–8] and are easily observed in CH_2Cl_2 solutions containing TBAP as supporting electrolyte.[8] Three stable, oxidized species can be stepwise generated from (OEP)Co in CH_2Cl_2 under CO, and each is characterized in this paper by UV–visible and FTIR spectroelectrochemistry. The resulting data are self-consistent and provide the first conclusive evidence for the formation of a $[(OEP)Co^{III}(CO)]^+$ complex in solution.

Experimental Section

Instrumentation and Procedure. Cyclic voltammograms were obtained with a PAR Model 273 potentiostat and an Omnigraphic 2000 X-Y recorder. A platinum button electrode with a surface area of 0.8 mm^2 was used as the working electrode. A homemade aqueous saturated calomel electrode (SCE) was used as the reference electrode and was separated from the bulk solution by a salt bridge filled with CH_2Cl_2 and 0.2 M tetrabutylammonium perchlorate (TBAP). A large surface area platinum electrode served as the auxiliary electrode.

A Matheson Model 8250 modular Dyna-Blender with flowmeter was used to deliver carbon monoxide/nitrogen mixtures that contained between 1 and 100% CO. The vapor pressure of methylene chloride (382 mmHg at 23 °C) was subtracted from the total pressure in calculating the partial pressure of CO.

In situ FTIR measurements were carried out with a light transparent spectroelectrochemical cell[9] by using an IBM IR32 spectrometer with an IBM 9000 computer system. The spectrum containing 0.2 M TBAP was taken as background to minimize matrix interferences.

UV–visible spectroelectrochemistry was carried out with a vacuum-tight thin-layer spectroelectrochemical cell that had a doublet platinum gauze working electrode.[10] A Tracor Northern TN-6500 multichannel analyzer was used for obtaining thin-layer UV–visible spectra.

High-purity N_2 was used to deoxygenate the solution before each experiment. All potentials are reported vs a saturated calomel electrode (SCE).

---

(1) Mu, X. H.; Kadish, K. M. *Inorg. Chem.* **1989**, *28*, 3743.
(2) Scholz, W. F.; Reed, C. A.; Lee, Y. J.; Scheidt, W. R.; Lang, G. *J. Am. Chem. Soc.* **1982**, *104*, 6791.
(3) Lin, X. Q.; Kadish, K. M. *Proc. Beijing Conf. Exhib. Instrum. Anal.* **1987**, *2*, 1311.
(4) Hinman, A. S.; Pavelich, B. J.; McGarty, K. *Can. J. Chem.* **1988**, *66*, 1589.
(5) Gasyna, Z.; Browett, W. R.; Stillman, M. J. *Inorg. Chem.* **1984**, *23*, 382.
(6) Itoh, K.; Nakahasi, K.; Toeda, H. *J. Phys. Chem.* **1988**, *92*, 1464.
(7) Shimomura, E. T.; Phillippi, M. A.; Goff, H. M.; Scholz, W. F.; Reed, C. A. *J. Am. Chem. Soc.* **1981**, *103*, 6778.
(8) Kadish, K. M.; Mu, X. H. *Pure Appl. Chem.* **1990**, *62*, 1051.
(9) Kadish, K. M.; Mu, X. H.; Lin, X. Q. *Electroanalysis* **1989**, *1*, 35.
(10) Lin, X. Q.; Kadish, K. M. *Anal. Chem.* **1985**, *57*, 1498.

0020-1669/91/1330-2444$02.50/0